

Article

# Precipitation Methods Using Calcium-Containing Ores for Fluoride Removal in Wastewater

Li Wang <sup>1,2</sup>, Ye Zhang <sup>1,2,\*</sup>, Ning Sun <sup>1,2</sup>, Wei Sun <sup>1,2</sup>, Yuehua Hu <sup>1,2</sup> and Honghu Tang <sup>1,2</sup><sup>1</sup> School of Minerals Processing and Bioengineering, Central South University, Changsha 410083, China<sup>2</sup> Key Laboratory of Hunan Province for Clean and Efficient Utilization of Strategic Calcium-Containing Mineral Resources, Central South University, Changsha 410083, China

\* Correspondence: zhangye94@csu.edu.cn; Tel.: +86-0731-8883-0482

Received: 26 July 2019; Accepted: 22 August 2019; Published: 24 August 2019



**Abstract:** F-containing wastewater does great harm to human health and the ecological environment and thus needs to be treated efficiently. In this paper, the new calcium-containing precipitant calcite and aided precipitant fluorite were adopted to purify F-containing wastewater. Relevant reaction conditions, such as reaction time, oscillation rate, dosage of hydrochloric acid, calcite dosage and the assisting sedimentation performance of fluorite, and action mechanism are analyzed. The experiment showed that the removal rate of fluoride in simulated wastewater reached 96.20%, when the reaction time, the dosage of calcite, the dosage of 5% dilute hydrochloric acid, and the oscillation rate was 30 min, 2 g/L, 21.76 g/L, and 160 r/min, respectively. Moreover, the removal rate of fluoride in the actual F-containing smelting wastewater reaches approximately 95% under the optimum condition of calcite dosage of 12 g/L, reaction time of 30 min, and oscillation rate of 160 r/min. The addition of fluorite significantly improves the sedimentation performance of the reactive precipitates. The experimental results showed that calcite and fluorite can effectively reduce the concentration of fluoride ions in F-containing wastewater and solve the problem of slow sedimentation of reactive precipitates.

**Keywords:** F-containing wastewater; precipitation method; calcite; fluorite

## 1. Introduction

Fluoride is a widely used industrial raw material. Fluoride generation is involved in the production processes in many industries [1–4]. The production and discharge of a large amount of F-containing wastewater has led to the continuous increase of the content of fluoride ion in natural water areas, which seriously pollutes the natural environment [5,6]. F-containing wastewater is mostly originated from fluoride containing “three wastes” produced by aluminum electrolysis, ceramics, cement, glass, semiconductor, steel, pharmaceutical, and other industries [7–10].

A wide range of industrial enterprises are involved in F-containing wastewater generation, and a large amount of F-containing wastewater is exported every year [11–14]. The fluoride concentration in industrial wastewater generally reaches up to hundreds or even thousands of milligrams of per liter and exceeds drastically the WHO (World Health Organization) guideline value of 1.5 mg/L in drinking water [15,16]. Moreover, F-containing wastewater is of great harm. The great amount of high-concentration F-containing wastewater discharged by factories is increasingly toxic to the environment and not only leads to human fluorosis but also seriously affects the natural ecosystem, making the ecosystem to lose balance and causing death and variation of aquatic organisms and plant [17–19].

F-containing wastewater can be treated by chemical precipitation method [20,21], coagulation and precipitation method [22,23], adsorption method [24–29], electrocoagulation method [20,30–33], reverse osmosis method [34–36], and ion exchange method [37,38]. Generally, chemicals such as

$\text{CaCl}_2$  and  $\text{CaO}$  are added for precipitating fluoride in wastewater. Zeng, Ling, Li, Luo, Sui and Guan [20] used 0.84 g/L  $\text{CaCl}_2$  to precipitate fluoride in synthetic water with 400 mg/L  $\text{F}^-$ , 15.2 mg/L  $\text{Ca}^{2+}$  and 2.16 mg/L  $\text{Mg}^{2+}$ , with high fluoride removal of 95.73%. Calcium hydroxide nanorods with dosage of 2 g/L were adopted for fluoride precipitation in acidic electroplating industrial wastewater containing 75 mg/L, with  $\text{F}^-$  removal of 91.7% [21]. The coagulation and precipitation methods remove  $\text{F}^-$  by adding a coagulant, such as iron salt (polyferric sulfate) and aluminum salt (polyaluminum sulfate), to produce a gelatinous substance. However, the single use of iron salt coagulants is not very effective and has a fluoride removal rate of only 10–30% [39]. Recently, a PAC-containing coagulant Actifluo was utilized for removing fluoride from pre-treated industrial glass and dye wastewater with  $\text{F}^-$  concentration of 15–30 mg/L [22]. And the  $\text{F}^-$  concentration could be decreased to below 3 mg/L by using 500–1500 mg/L Actifluo. Additionally, the  $\text{F}^-$  concentration of simulated fluoride-polluted water could be reduced from approximately 5 mg/L to below 1.5 mg/L by using only 20 mg/L Al-based coagulant PSiFAC-Mg<sub>30-10-15</sub> [23]. The adsorption method is generally suitable for the treatment of low-fluoride wastewater. For the treatment of high-concentration F-containing wastewater, pretreatment by precipitation method is necessary. Otherwise, the adsorbent should be continuously regenerated so that the operating cost of the equipment can be increased. Reverse osmosis technology is one of the membrane separation technologies that has been rapidly developed in recent years. High pressure is used to separate water molecules in high-concentration wastewater from other components through a reverse osmosis membrane. However, owing to the high market price of semipermeable membranes, the application cost of reverse osmosis technology is relatively high. Meanwhile, raw water quality is of relatively high requirement. It should be pretreated generally.

The chemical precipitation method is a simple process, low in cost, and widely used for fluoride removal. F-containing wastewater of high concentration usually exhibits strong acidity (pH = 1–2). Therefore, fluoride ions can be removed by precipitation with calcium ions, and in the meantime wastewater can be neutralized by adding lime or other calcium salts. Gao, et al. [40] designed a process improvement plan for “slaked lime sedimentation-water recycling” for solving the problem of excessive fluoride content in wastewater from the phosphate plant. The results showed that when the dosage of slaked lime is 1.3 times the theoretical mass and the reaction time is 0.5 h, the fluoride concentration can be decreased below 30 mg/L. However, the great disadvantage of this method is that the sedimentation process of precipitates is very slow.

In this paper, the new calcium-containing precipitant calcite and aided precipitant fluorite are adopted to purify F-containing wastewater, which represents a new approach for fluoride removal from F-containing wastewater. As well, several measures are taken in order to explore the relevant mechanisms of precipitation and sedimentation process.

## 2. Experimental Section

### 2.1. Experimental Materials

The simulated wastewater water sample in the experiment was prepared by sodium fluoride and deionized water at  $\text{F}^-$  concentration of 300 mg/L, with pH of 6.60. The preparation method is as follows: The sodium fluoride was dried in an oven at 90 °C for 3 h. After cooling, 0.6632 g sodium fluoride was weighed accurately using an electronic balance, placed in a clean 50 mL beaker and dissolved in deionized water. Then, it was moved into a 1 L volumetric flask by a glass rod, and the beaker and glass rod were washed for 4–5 times with deionized water. The washing solution was transferred to the volumetric flask and diluted to the mark with deionized water. The prepared solution was set aside for later use.

The actual F-containing wastewater used in the experiment was from a smelting plant in Xiamen. The  $\text{F}^-$  concentration was about 310 mg/L, and the pH was 2.08. The composition of actual F-containing smelting wastewater is shown in Table 1. The calcite and fluorite used in the experiments were taken from Hunan province, China, with the purity of 97.54% and 98.89% respectively. The pure calcite and

fluorite minerals were ground using a ball mill of corundum to  $-74 \mu\text{m} \sim +38 \mu\text{m}$  and  $-150 \mu\text{m} \sim +74 \mu\text{m}$ , respectively.

**Table 1.** The composition of actual F-containing smelting wastewater.

Parameters	pH	COD	F <sup>-</sup>	Cl <sup>-</sup>	SO <sub>4</sub> <sup>2-</sup>	Na <sup>+</sup>	K <sup>+</sup>
Concentration (mg/L)	2.08	8	310	3326.40	1673.20	26.38	537.70
Parameters	Ni <sup>+</sup>	NH <sub>4</sub> <sup>+</sup>	Ca <sup>2+</sup>	Mg <sup>2+</sup>	Pb <sup>2+</sup>	Cu <sup>2+</sup>	
Concentration (mg/L)	1.53	9.62	0.66	4.21	15.72	2.94	

## 2.2. Precipitation Experiment

50 mL of F-containing wastewater sample (300 mg/L) was placed exactly in a 150 mL Erlenmeyer flask on a digital water-bath constant temperature oscillator (SHA-82A, Changzhou Putian Instrument Manufacturing Co., Ltd., Changzhou, China) for oscillating. Then, a part of the solution was transferred to a desktop high-speed centrifuge (TG16-WS type, Hunan Xiangyi Laboratory Instrument Development Co., Ltd., Changsha, China). The residual concentration of the supernatant after centrifugation was measured by fluoride ion selective electrode method. The pH of the solutions was adjusted by using dilute HCl and NaOH solutions.

## 2.3. Determination of Fluoride Ion Concentration

The commonly used methods for measuring fluoride ion concentration in water samples are ion chromatography, fluoride reagent colorimetry, and fluoride ion selective electrode. The advantages of fluoride ion selective electrode method are easy operation, simple equipment, good selectivity, high accuracy, small influence on water sample turbidity and chromaticity, and wide measurement concentration range (0.05–1900 mg/L). Therefore, it is widely used. The fluoride ion selective electrode method was adopted to determine the F<sup>-</sup> concentration in wastewater in this paper. Fluoride ion concentration was measured according to the analysis standard of the International Organization for Standardization [41] with a fluoride ion selective electrode (PF-1-01, Shanghai INESA Scientific Instrument Co., Ltd., Shanghai, China), reference electrode (232, Shanghai INESA Scientific Instrument Co., Ltd., Shanghai, China) and lightning magnetic pH meter (pHS-3C, Shanghai INESA Scientific Instrument Co., Ltd., Shanghai, China). First of all, TISAB (Total Ionic Strength Adjustment Buffer) solution was prepared using deionized water, CH<sub>3</sub>COOH, NaCl, CDTA, and NaOH. Then, four standard solution with F<sup>-</sup> concentration of 10<sup>-2</sup>, 10<sup>-3</sup>, 10<sup>-4</sup>, 10<sup>-5</sup> mol/L and TISAB were mixed with equal volume and the potentials of mixed solution were measured by inserting fluoride ion selective electrode and reference electrode into solution in order to construct the calibration curve. Finally, the sample solution was diluted with equal volume of TISAB solution and the potential mixed solution was measured. The F<sup>-</sup> concentration of sample solution could be obtained according to the calibration curve.

## 2.4. Analysis Methods

An X-Ray diffractometer (D8 Advance, Bruker, Karlsruhe, Germany) with rotating Cu anode was used for mineral phase identification. MDI Jade 6 software (6.0, Materials Data, Inc., Livermore, CA, USA) was used for the assignment of all diffraction peaks by reference to PDF-2004 standard cards. The morphologies and surface elements analysis of the precipitates were characterized using a scanning electron microscope (SEM; Nova Nano SEM230, FEI Electron Optics B.V, Brno, Czech Republic) coupled with EDS (FEI Electron Optics B.V, Brno, Czech Republic).

### 3. Results and Discussion

#### 3.1. Precipitation Experiments in Simulated System

The influences of reaction time (a), dosage of calcite (b), dosage of hydrochloric acid (c), and oscillation rate (d) on fluoride removal process by calcite are shown in Figure 1. As shown in Figure 1a, the fluoride concentration decreasing quickly from 300 mg/L to approximately 8 mg/L and the residual fluoride ion concentration in the wastewater was hardly changed with the reaction time extending, indicating that calcite and hydrochloric acid can act quickly to release calcium ions and form precipitates with fluoride ions after hydrochloric acid was added to the wastewater. As calcite is insoluble in water, fluoride cannot be effectively removed by adding water directly under neutral conditions. A certain amount of acid is necessary to dissolve calcite in order to produce  $\text{Ca}^{2+}$ , which could precipitate fluoride ions.  $\text{CO}_2$  was produced during the dissolution process and was dissolved in water. Figure 2 shows the XRD diffraction pattern of untreated calcite (a) and the precipitation product (b). The diffraction peak of  $\text{CaF}_2$  was detected in the calcite precipitation product, indicating that  $\text{CaF}_2$  was produced in the calcite precipitation reaction process. The reaction time poses small influence on fluoride removal by calcite precipitation method. Therefore, the reaction time was selected at 30 min.

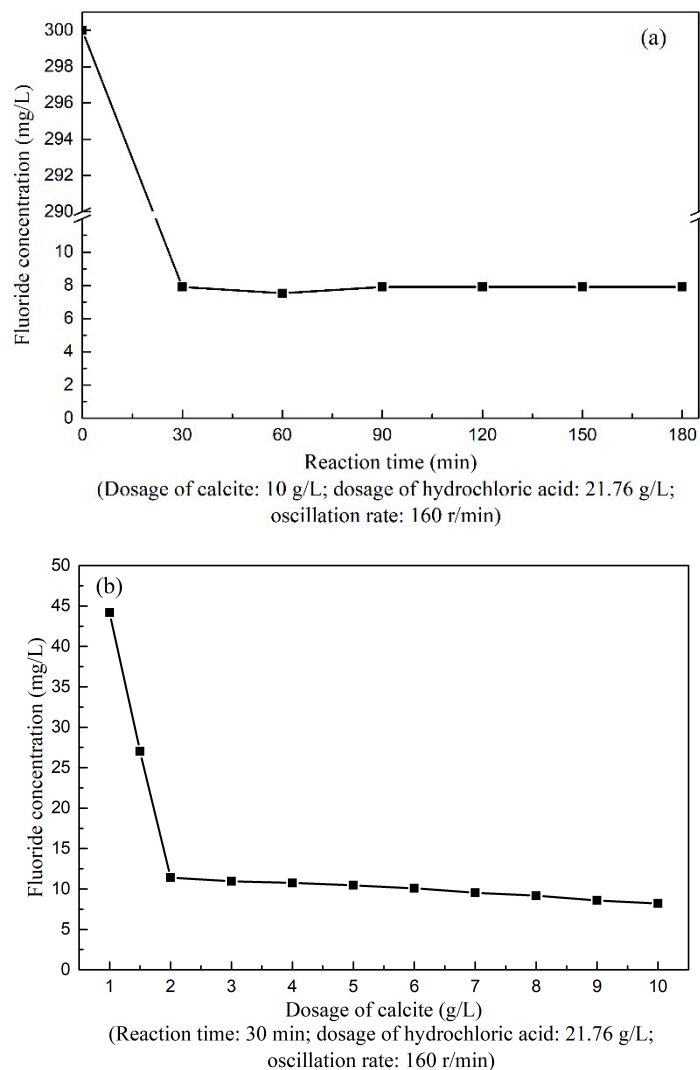
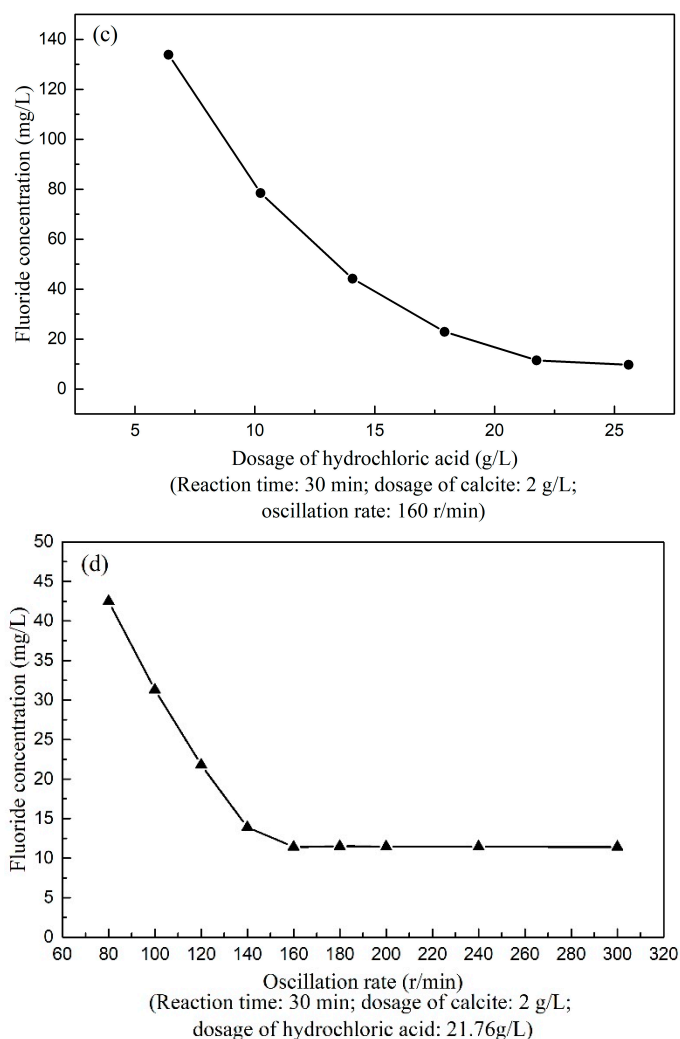
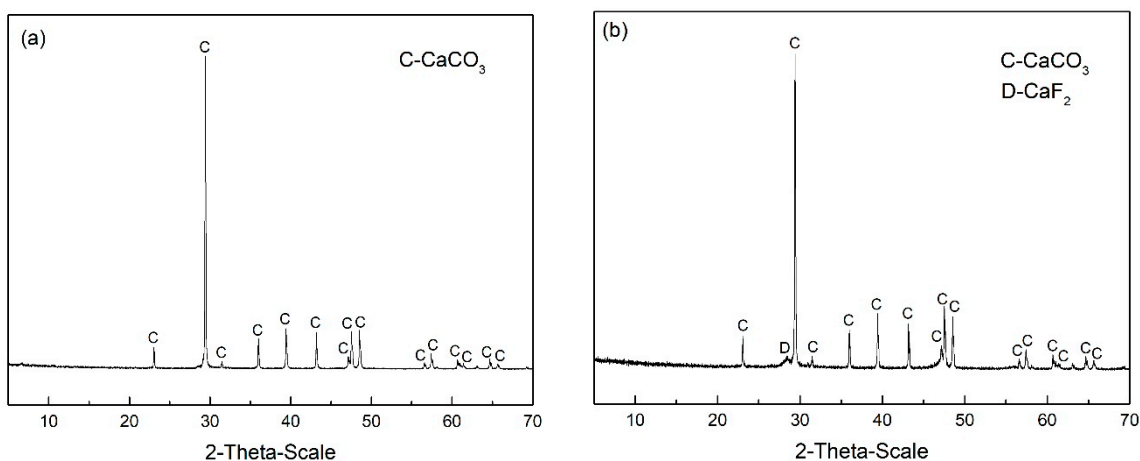


Figure 1. Cont.



**Figure 1.** Influence of reaction time (a), dosage of calcite (b), dosage of hydrochloric acid (c), and oscillation rate (d) on fluoride removal process from simulated wastewater by calcite.



**Figure 2.** XRD pattern of the calcite (a) and the precipitation product (b).

It can be seen from Figure 1b that as the dosage of calcite increased from 1 g/L to 2 g/L, the residual F<sup>-</sup> concentration decreased rapidly. This is because the Ca<sup>2+</sup> formed by calcite and hydrochloric acid reacted quickly with the F<sup>-</sup>. While as the dosage of calcite exceeded 2 g/L, the residual F<sup>-</sup> concentration

reduced slowly. Since when the dosage of calcite reached 2 g/L, the residual  $F^-$  concentration in wastewater dropped to 11.41 mg/L, and the removal rate reached 96.20%. As reported in several studies [42,43], when the fluoride concentration is lower ( $< \sim 10$  mg/L), the fluoride adsorption on the surface of calcite may play a dominant role. When the calcite dosage exceeded 2 g/L, the fluoride adsorption of excessive calcite become dominant. Moreover, the adsorption capacity of calcite is relatively low. Therefore, the  $F^-$  concentration in wastewater decreased slowly. As the  $F^-$  concentration in wastewater can be reduced to less than 12 mg/L by controlling the dosage of calcite at more than 2 g/L. Therefore, the optimum calcite dosage was determined as 2 g/L. Compared with experiments reported by Zeng, Ling, Li, Luo, Sui and Guan [20], who used 0.84 g/L  $CaCl_2$  to remove 95.73% of fluoride in synthetic water with 400 mg/L  $F^-$ , the dosage of calcite is a little higher than that of  $CaCl_2$  but the unit cost of calcite is quite lower than that of  $CaCl_2$  as a function of the online quotation. In terms of the removal efficiency and cost of reagent, calcite exhibits great potential for fluoride removal from wastewater with high fluoride concentration.

The effect of dosage of hydrochloric acid on the fluoride is shown in Figure 1c. It is illustrated that the residual  $F^-$  concentration decreased rapidly with the growth of the dosage of hydrochloric acid, indicating that the added hydrochloric acid reacted with calcite to form  $Ca^{2+}$ , which precipitated the  $F^-$  in wastewater. Moreover, a large amount of  $H^+$  could react with calcite with the increase of hydrochloric acid dosage. When the dosage of hydrochloric acid exceeded 21.76 g/L, the residual  $F^-$  concentration in wastewater decreased to 11.48 mg/L. Therefore, the concentration in the water can be reduced to less than 12 mg/L by controlling the dosage of hydrochloric acid at about 21.76 g/L. However, hydrochloric acid should not be added excessively or it will disrupt subsequent neutralization operations. Therefore, the dosage of hydrochloric acid was selected as 21.76 g/L.

As shown Figure 1d, as the oscillation rate increased, and the concentration of the residual  $F^-$  gradually decreased. When the oscillation rate was higher than 160 r/min, the residual  $F^-$  concentration decreased slowly and gradually stabilized with the increase of oscillation rate. Therefore, a certain oscillation rate is necessary in order to prevent newly formed calcium fluoride precipitates from adhering to the calcite surface, which can ensure the normal reaction of calcite and acid. By this way, the content of effective calcium ions in the water sample would not change too much. On the other hand, the reaction efficiency between calcite and hydrochloric acid can be improved and the process of fluoride removal can be promoted. Hence, the optimum oscillation rate was 160 r/min. In conclusion, the fluoride in simulated wastewater could be removed by 96.20%, under the optimized condition of reaction time of 30 min, calcite dosage of 2 g/L, hydrochloric acid dosage of 21.76 g/L, and oscillation rate of 160 r/min.

### 3.2. Effect of Fluorite on Sedimentation Performance

As shown in Figure 3 the sedimentation process of the reactive precipitates was slow without addition of fluorite. While under the condition of adding fluorite, the reactive precipitates can be quickly settled within 30 min (see in Figure 4). This may be due to the fact that the growth of precipitation products on the added fluorite promoted the sedimentation of precipitates. As is known, precipitation is a process involving mass transfer, chemical reaction, as well as crystallization, it is typically operated at high supersaturation levels which lead to fast nucleation rates [44,45]. However, this fast nucleation rates generally results in formation of small crystals, which settle very slowly in the solution [46,47]. Generally, the seed crystals are introduced in order to induce nucleation of the solid phase at a slow and controlled rate, which is conducive to grow the macroscopic crystals [48,49]. Therefore, in this sedimentation test, the  $CaF_2$  particles generated by the precipitation reaction were too small to settle quickly without addition of fluorite. While under the condition of adding fluorites, the small  $CaF_2$  particles took the added fluorites as the nucleus and grow on their surface. The particle size of the suspended particles in the solution increased, thereby increasing the sedimentation speed.

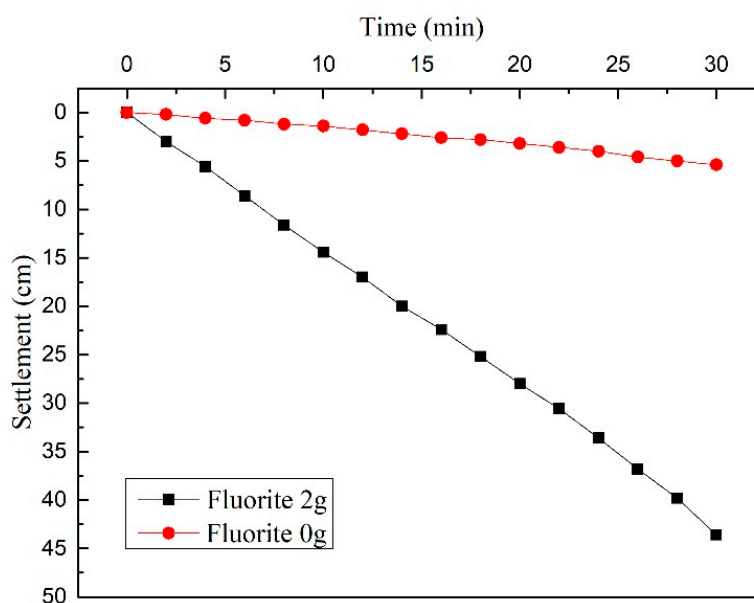


**Figure 3.** Sedimentation test results when fluorite is added at 0 g and 2 g. (Reaction time: 30 min; dosage of calcite: 2 g/L; dosage of hydrochloric acid: 21.76 g/L; oscillation rate: 160 r/min).

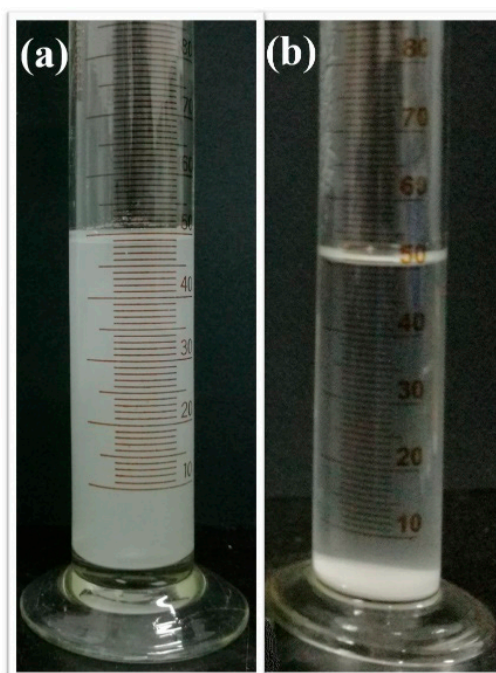


**Figure 4.** Sedimentation diagram before (a) and after (b) fluorite addition.

This phenomenon could also be demonstrated by the SEM analysis. The SEM analysis was performed before and after the addition of fluorite. Figure 5a,b are the scanning electron micrographs of the products obtained before and after fluorite addition, respectively. The scanning electron micrographs of the two samples were compared, and the result showed that many “small white spots” appeared on the surface of the product obtained after the addition of fluorite. Figure 5c showed the energy spectrum of the “small white spots” on the fluorite surface. As shown in Figure 5c, the “small white spots” are  $\text{CaF}_2$ , indicating that calcium fluoride particles formed by precipitation reaction adhere to the surface of the fluorite and descended with fluorite rapidly. As a result, the sedimentation speed of precipitation products was accelerated by adding fluorite.

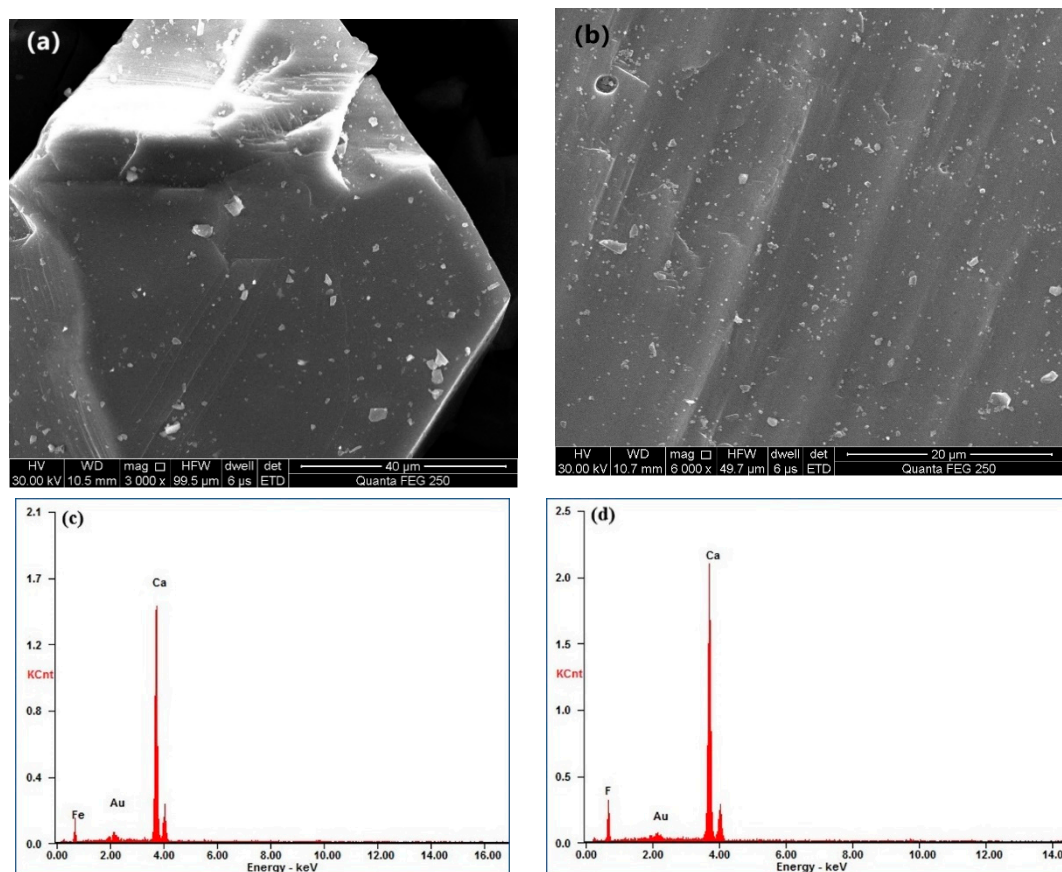


**Figure 5.** Scanning electron micrograph before (a) and after (b) fluorite addition and EDS diagram before (c) and after (d) fluorite addition.

Fluorite, as a precipitation assistant, can effectively accelerate the sedimentation rate of calcite precipitation reaction products because fluorite has a much larger particle size than the  $\text{CaF}_2$  particles produced by the precipitation reaction. Therefore, fluorite can be used as a nucleus to which  $\text{CaF}_2$  precipitates particles adhere, and these  $\text{CaF}_2$  precipitates particles can aggregate on the surface of fluorite to quickly settle with fluorite.

### 3.3. Precipitation Experiments in Actual System

The precipitation experiments of actual F-containing smelting wastewater was conducted and several influence factors were investigated such as pH, reaction time, dosage of calcite, and oscillation rate. The parameters of the actual smelting wastewater are shown in Table 1. The influences of pH, reaction time, dosage of calcite, and oscillation rate on the fluoride removal from actual smelting wastewater are shown in Figure 6.

It is illustrated in the Figure 6a that the fluoride concentration reduced rapidly with the decrease of the solution pH. The solution pH played an important role in fluoride removal from actual F-containing wastewater. It is just like the reaction between HCl and calcite in simulated wastewater. Under the lower pH condition, calcite could react with  $\text{H}^+$  in actual wastewater to form  $\text{Ca}^{2+}$  and hence the  $\text{F}^-$  could be precipitated by  $\text{Ca}^{2+}$ . When the solution pH was approximately 2, the fluoride concentration reduced to below 20 mg/L. As well, the residual  $\text{F}^-$  concentration remained stable after further lowering the pH. Since the pH of actual F-containing wastewater was 2.08, no HCl needed to be added in this actual wastewater.



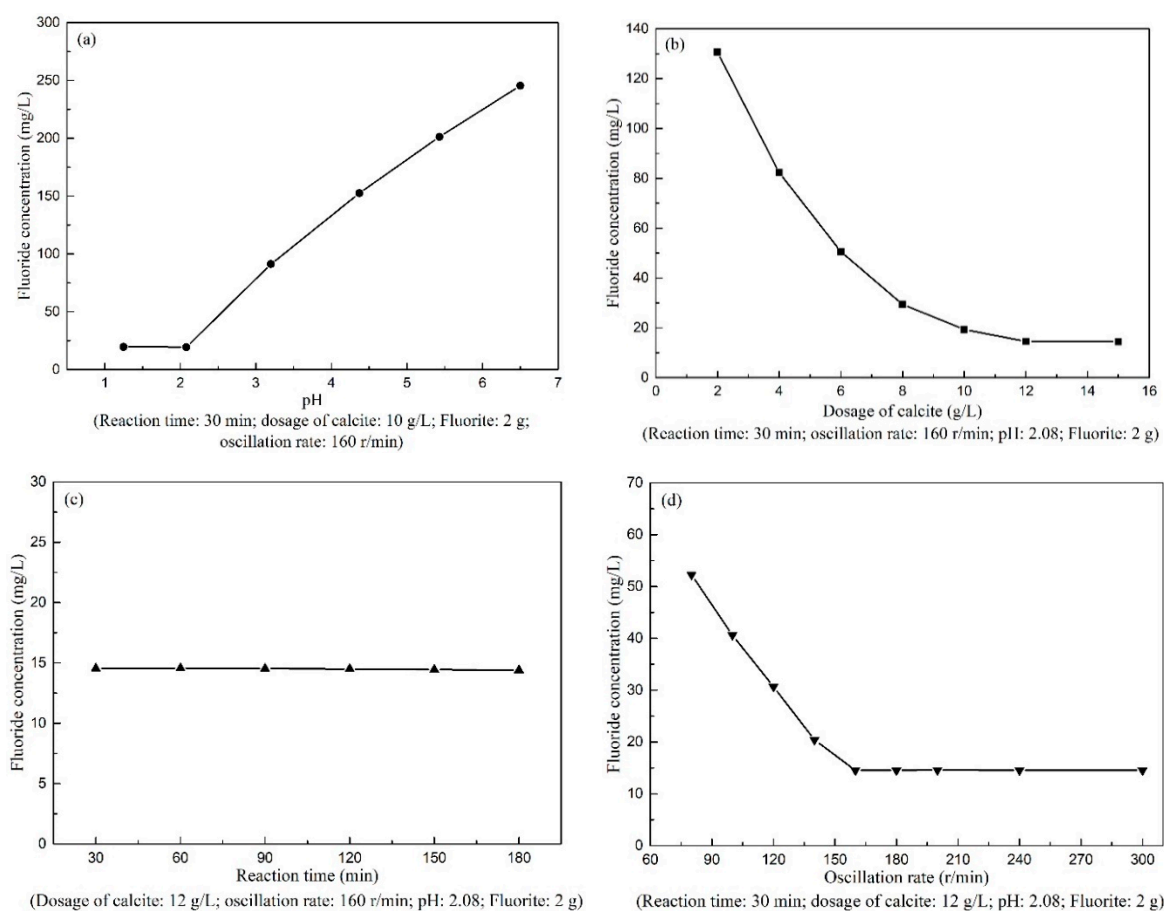


**Figure 6.** Influence of pH (a), dosage of calcite (b), reaction time (c), and oscillation rate (d) on fluoride removal process from actual wastewater by calcite.

The impact of dosage of calcite on fluoride removal from actual wastewater was shown in Figure 6b. It is shown that with the growth of calcite dosage, the residual fluoride concentration had a gradual decrease, followed by keeping steady. The fluoride concentration could decrease from 310 mg/L to approximately 14.5 mg/L at the calcite dosage of 12 g/L, with the fluoride removal rate of 95.32%. This is different from the results obtained in simulated system, where the fluoride concentration could reduce to less than 12 mg/L at the calcite dosage of 2 g/L and even to approximately 8 mg/L at the calcite dosage of 10 g/L. This is probably because the ionic strength of actual wastewater is higher than that of simulated wastewater. Moreover, the high ionic strength upgrades the degree of aggregation of outer precipitation products on calcite and in turn depresses the reaction between  $H^+$  and calcite [50,51]. Therefore, more calcite was needed in the actual system than in the simulated wastewater. Nonetheless, considering that the cost of calcite is quite lower than of  $CaCl_2$  and  $CaO$ , the calcite exhibited great potential for fluoride removal.

The influences of reaction time and oscillation rate are shown in Figure 6c and 6d respectively. Just like the results obtained from the simulated system, the reaction time almost had no influence on the fluoride by calcite. As for the impact of oscillation rate, it is illustrated in Figure 6d that the variation tendency of fluoride concentration was similar to that in the simulated system. The optimum oscillation rate was also selected as 160 r/min, where the fluoride removal rate could reach around 95%. As a consequence, the fluoride in actual wastewater could be removed by approximately 95%, under the optimum condition of calcite dosage of 12 g/L, pH of 2.08, reaction time of 30 min, oscillation rate of 160 r/min, and 2 g fluorite.

#### 4. Conclusions

In this paper, new precipitant calcite and aided precipitant fluorite were adopted to purify F-containing wastewater. Relevant reaction conditions, such as reaction time, oscillation rate, dosage of hydrochloric acid, calcite dosage, and the assisting sedimentation performance of fluorite are explored, and the reaction mechanism were discussed. It could be found from the experiments that calcite can effectively remove fluoride in F-containing wastewater. The dosage of precipitant, oscillation rate, and dosage of acid pose important influences on the removal of fluoride. On the other hand, fluorite can effectively improve the sedimentation of the reactive precipitates. SEM results showed that the reactive precipitates  $\text{CaF}_2$  can grow on the surface of fluorite and sedimentation performance was improved accordingly. Under optimal experimental conditions of reaction time of 30min, calcite dosage of 2 g/L, hydrochloric acid dosage of 21.76 g/L, oscillation rate of 160 r/min, and 2 g fluorite, the removal rate of fluoride in the simulated F-containing wastewater reached 96.20% and the precipitation products could settle quickly. Moreover, the removal rate of fluoride in the actual F-containing smelting wastewater reached 95% at the optimum condition of calcite dosage of 12 g/L, pH of 2.08, reaction time of 30 min, oscillation rate of 160 r/min, and 2 g fluorite. The experiment showed that the precipitant calcite can effectively reduce the concentration of fluoride ion in F-containing wastewater and the aided precipitant fluorite can solve the problem of slow sedimentation of reactive precipitates.

**Author Contributions:** Conceptualization, W.S. and Y.H.; Methodology, L.W. and Y.Z.; Formal analysis, H.T.; Investigation, Y.Z. and N.S.; Writing—original draft preparation, L.W. and Y.Z.; Writing—review and editing, L.W. and Y.Z.

**Funding:** This research was funded by the National Key R&D Program of China (2018YFC1901901), the National Natural Science Foundation of China (51704329, 51705540), the Innovation Driven Plan of Central South University (No. 2015CX005), the National 111 Project (No. B14034), the Open Sharing Fund for the Large-scale Instruments and Equipments of Central South University and the Collaborative Innovation Center for Clean and Efficient Utilization of Strategic Metal Mineral Resources.

**Conflicts of Interest:** The authors declare no conflict of interest.

#### References

1. Xu, L.; Chen, G.; Peng, C.; Qiao, H.; Ke, F.; Hou, R.; Li, D.; Cai, H.; Wan, X. Adsorptive removal of fluoride from drinking water using porous starch loaded with common metal ions. *Carbohydr. Polym.* **2017**, *160*, 82–89. [[CrossRef](#)] [[PubMed](#)]
2. Zhang, Y.X.; Jia, Y. Fluoride adsorption onto amorphous aluminum hydroxide: Roles of the surface acetate anions. *J. Colloid Interface Sci.* **2016**, *483*, 295–306. [[CrossRef](#)] [[PubMed](#)]
3. Zhang, Y.; Hu, Y.H.; Sun, N.; Liu, R.Q.; Wang, Z.; Wang, L.; Sun, W. Systematic review of feldspar beneficiation and its comprehensive application. *Miner. Eng.* **2018**, *128*, 141–152. [[CrossRef](#)]
4. Lyu, F.; Gao, J.; Sun, N.; Liu, R.; Sun, X.; Cao, X.; Wang, L.; Sun, W. Utilisation of propyl gallate as a novel selective collector for diasporite flotation. *Miner. Eng.* **2019**, *131*, 66–72. [[CrossRef](#)]
5. Silva, J.F.A.; Graça, N.S.; Ribeiro, A.M.; Rodrigues, A.E. Electrocoagulation process for the removal of co-existent fluoride, arsenic and iron from contaminated drinking water. *Sep. Purif. Technol.* **2018**, *197*, 237–243. [[CrossRef](#)]
6. Aoudj, S.; Khelifa, A.; Drouiche, N. Removal of fluoride, sds, ammonia and turbidity from semiconductor wastewater by combined electrocoagulation-electroflotation. *Chemosphere* **2017**, *180*, 379–387. [[CrossRef](#)] [[PubMed](#)]
7. Vázquez-Guerrero, A.; Alfaro-Cuevas-Villanueva, R.; Rutiaga-Quñones, J.G.; Cortés-Martínez, R. Fluoride removal by aluminum-modified pine sawdust: Effect of competitive ions. *Ecol. Eng.* **2016**, *94*, 365–379. [[CrossRef](#)]
8. Zhang, Y.; Hu, Y.H.; Sun, N.; Khoso, S.A.; Wang, L.; Sun, W. A novel precipitant for separating lithium from magnesium in high Mg/Li ratio brine. *Hydrometallurgy* **2019**, *187*, 125–133. [[CrossRef](#)]
9. Zhang, Y.; Hu, Y.; Wang, L.; Sun, W. Systematic review of lithium extraction from salt-lake brines via precipitation approaches. *Miner. Eng.* **2019**, 105868. [[CrossRef](#)]

10. Li, Y.; Jiang, Y.; Wang, T.J.; Zhang, C.; Wang, H. Performance of fluoride electrosorption using micropore-dominant activated carbon as an electrode. *Sep. Purif. Technol.* **2017**, *172*, 415–421. [[CrossRef](#)]
11. Zhang, Y.; Lin, X.; Zhou, Q.; Luo, X. Fluoride adsorption from aqueous solution by magnetic core-shell Fe<sub>3</sub>O<sub>4</sub>@alginate-La particles fabricated via electro-coextrusion. *Appl. Surf. Sci.* **2016**, *389*, 34–45. [[CrossRef](#)]
12. Guan, Q.J.; Sun, W.; Hu, Y.H.; Yin, Z.G.; Zhang, C.H.; Guan, C.P.; Zhu, X.N.; Khoso, S.A. Simultaneous control of particle size and morphology of  $\alpha$ -CaSO<sub>4</sub>· $\frac{1}{2}$ H<sub>2</sub>O with organic additives. *J. Am. Ceram. Soc.* **2018**, *102*, 2440–2450.
13. Ye, Q.; Li, G.H.; Deng, B.N.; Lun, J.; Rao, M.J.; Peng, Z.W.; Zhang, Y.B.; Jiang, T. Solvent extraction behavior of metal ions and selective separation Sc<sup>3+</sup> in phosphoric acid medium using P<sub>2</sub>O<sub>4</sub>. *Sep. Purif. Technol.* **2019**, *209*, 175–181. [[CrossRef](#)]
14. Thakur, L.S.; Mondal, P. Simultaneous arsenic and fluoride removal from synthetic and real groundwater by electrocoagulation process: Parametric and cost evaluation. *J. Environ. Manag.* **2017**, *190*, 102–112. [[CrossRef](#)]
15. Tang, W.; Kovalsky, P.; Cao, B.; Waite, T.D. Investigation of fluoride removal from low-salinity groundwater by single-pass constant-voltage capacitive deionization. *Water Res.* **2016**, *99*, 112–121. [[CrossRef](#)] [[PubMed](#)]
16. Liu, Y.; Fan, Q.; Wang, S.; Liu, Y.; Zhou, A.; Fan, L. Adsorptive removal of fluoride from aqueous solutions using Al-humic acid-La aerogel composites. *Chem. Eng. J.* **2016**, *306*, 174–185. [[CrossRef](#)]
17. Tang, W.; Kovalsky, P.; He, D.; Waite, T.D. Fluoride and nitrate removal from brackish groundwaters by batch-mode capacitive deionization. *Water Res.* **2015**, *84*, 342–349. [[CrossRef](#)]
18. Wang, L.; Sun, N.; Wang, Z.; Han, H.; Yang, Y.; Liu, R.; Hu, Y.; Tang, H.; Sun, W. Self-assembly of mixed dodecylamine–dodecanol molecules at the air/water interface based on large-scale molecular dynamics. *J. Mol. Liq.* **2019**, *276*, 867–874. [[CrossRef](#)]
19. Claveau-Mallet, D.; Wallace, S.; Comeau, Y. Removal of phosphorus, fluoride and metals from a gypsum mining leachate using steel slag filters. *Water Res.* **2013**, *47*, 1512–1520. [[CrossRef](#)]
20. Zeng, G.; Ling, B.; Li, Z.; Luo, S.; Sui, X.; Guan, Q. Fluorine removal and calcium fluoride recovery from rare-earth smelting wastewater using fluidized bed crystallization process. *J. Hazard Mater.* **2019**, *373*, 313–320. [[CrossRef](#)]
21. Chaudhary, M.; Maiti, A. Defluoridation by highly efficient calcium hydroxide nanorods from synthetic and industrial wastewater. *Colloids Surf. A* **2019**, *561*, 79–88. [[CrossRef](#)]
22. Venditti, F.; Cuomo, F.; Giansalvo, G.; Giustini, M.; Cinelli, G.; Lopez, F. Fluorides decontamination by means of aluminum polychloride based commercial coagulant. *J. Water Process Eng.* **2018**, *26*, 182–186. [[CrossRef](#)]
23. Tolkou, A.K.; Mitrakas, M.; Katsoyiannis, I.A.; Ernst, M.; Zouboulis, A.I. Fluoride removal from water by composite Al/Fe/Si/Mg pre-polymerized coagulants: Characterization and application. *Chemosphere* **2019**, *231*, 528–537. [[CrossRef](#)]
24. Robshaw, T.; Tukra, S.; Hammond, D.B.; Leggett, G.J.; Ogden, M.D. Highly efficient fluoride extraction from simulant leachate of spent potlining via La-loaded chelating resin. An equilibrium study. *J. Hazard Mater.* **2019**, *361*, 200–209. [[CrossRef](#)]
25. Raghav, S.; Nehra, S.; Kumar, D. Adsorptive removal studies of fluoride in aqueous system by bimetallic oxide incorporated in cellulose. *Process Saf. Environ.* **2019**, *127*, 211–225. [[CrossRef](#)]
26. Mullick, A.; Neogi, S. Ultrasound assisted synthesis of Mg-Mn-Zr impregnated activated carbon for effective fluoride adsorption from water. *Ultrason. Sonochem.* **2019**, *50*, 126–137. [[CrossRef](#)]
27. Luo, S.; Guo, Y.; Yang, Y.; Zhou, X.; Peng, L.; Wu, X.; Zeng, Q. Synthesis of calcined La-doped layered double hydroxides and application on simultaneously removal of arsenate and fluoride. *J. Solid State Chem.* **2019**, *275*, 197–205. [[CrossRef](#)]
28. Zhou, J.; Zhu, W.; Yu, J.; Zhang, H.; Zhang, Y.; Lin, X.; Luo, X. Highly selective and efficient removal of fluoride from ground water by layered Al-Zr-La Tri-metal hydroxide. *Appl. Surf. Sci.* **2018**, *435*, 920–927. [[CrossRef](#)]
29. Chigondo, M.; Kamdem Paumo, H.; Bhaumik, M.; Pillay, K.; Maity, A. Hydrous CeO<sub>2</sub>–Fe<sub>3</sub>O<sub>4</sub> decorated polyaniline fibers nanocomposite for effective defluoridation of drinking water. *J. Colloid Interface Sci.* **2018**, *532*, 500–516. [[CrossRef](#)]
30. Hashim, K.S.; Shaw, A.; Al Khaddar, R.; Ortoneda Pedrola, M.; Phipps, D. Defluoridation of drinking water using a new flow column-electrocoagulation reactor (FCER)-experimental, statistical, and economic approach. *J. Environ. Manag.* **2017**, *197*, 80–88. [[CrossRef](#)]

31. Cui, H.; Qian, Y.; An, H.; Sun, C.; Zhai, J.; Li, Q. Electrochemical removal of fluoride from water by paoa-modified carbon felt electrodes in a continuous flow reactor. *Water Res.* **2012**, *46*, 3943–3950. [CrossRef]
32. Hu, C.Y.; Lo, S.L.; Kuan, W.H.; Lee, Y.D. Removal of fluoride from semiconductor wastewater by electrocoagulation-flotation. *Water Res.* **2005**, *39*, 895–901. [CrossRef]
33. Lin, J.Y.; Raharjo, A.; Hsu, L.H.; Shih, Y.J.; Huang, Y.H. Electrocoagulation of tetrafluoroborate ( $\text{BF}_4^-$ ) and the derived boron and fluorine using aluminum electrodes. *Water Res.* **2019**, *155*, 362–371. [CrossRef]
34. Yadav, K.K.; Kumar, S.; Pham, Q.B.; Gupta, N.; Rezania, S.; Kamyab, H.; Yadav, S.; Vymazal, J.; Kumar, V.; Tri, D.Q.; et al. Fluoride contamination, health problems and remediation methods in Asian groundwater: A comprehensive review. *Ecotoxicol. Environ. Saf.* **2019**, *182*, 109362. [CrossRef]
35. Jeihanipour, A.; Shen, J.; Abbt-Braun, G.; Huber, S.A.; Mkongo, G.; Schafer, A.I. Seasonal variation of organic matter characteristics and fluoride concentration in the Maji ya Chai River (Tanzania): Impact on treatability by nanofiltration/reverse osmosis. *Sci. Total Environ.* **2018**, *637–638*, 1209–1220. [CrossRef]
36. Grzegorzec, M.; Majewska-Nowak, K. The use of micellar-enhanced ultrafiltration (MEUF) for fluoride removal from aqueous solutions. *Sep. Purif. Technol.* **2018**, *195*, 1–11. [CrossRef]
37. Herath, H.; Kawakami, T.; Tafu, M. Repeated heat regeneration of bone char for sustainable use in fluoride removal from drinking water. *Healthcare* **2018**, *6*, 143. [CrossRef]
38. Asimeng, B.O.; Fianko, J.R.; Kaufmann, E.E.; Tiburu, E.K.; Hayford, C.F.; Anani, P.A.; Dzikunu, O.K. Preparation and characterization of hydroxyapatite from achatina achatina snail shells: Effect of carbonate substitution and trace elements on defluoridation of water. *J. Asian Ceram. Soc.* **2018**, *6*, 205–212. [CrossRef]
39. Zhang, Y. Study on New Technology about Coprocessing High-Acid Wastewater Containing Fluoride by Using Calcium-Based Ore. Master's Thesis, Central South University, Changsha, China, 2017.
40. Gao, H.; Li, R.; Fan, C. Treatment of acidic fluoride-containing wastewater by chemical sedimentation process. *Technol. Water Treat.* **2014**, *40*, 107–110, 114.
41. ISO. *Dentistry—Analysis of Fluoride Concentration in Aqueous Solutions by Use of Fluoride Ion-Selective Electrode*; International Standardization Organization: Geneva, Switzerland, 2018.
42. Budyanto, S.; Kuo, Y.-L.; Liu, J.C. Adsorption and precipitation of fluoride on calcite nanoparticles: A spectroscopic study. *Sep. Purif. Technol.* **2015**, *150*, 325–331. [CrossRef]
43. Padhi, S.; Tokunaga, T. Surface complexation modeling of fluoride sorption onto calcite. *J. Environ. Chem. Eng.* **2015**, *3*, 1892–1900. [CrossRef]
44. Claassen, J.O.; Sandenbergh, R.F. Particle growth parameters in the precipitation of metastable iron phases from zinc-rich solutions. *Hydrometallurgy* **2006**, *84*, 165–174. [CrossRef]
45. Wachi, S.; Jones, A.G. Mass transfer with chemical reaction and precipitation. *Chem. Eng. Sci.* **1991**, *46*, 1027–1033. [CrossRef]
46. Huang, Y.-F.; Kao, H.-L.; Ruan, J.; Su, A.-C. Effects of solution status on single-crystal growth habit of poly(l-lactide). *Macromolecules* **2010**, *43*, 7222–7227. [CrossRef]
47. De Yoreo, J.J. Principles of crystal nucleation and growth. *Rev. Mineral. Geochem.* **2003**, *54*, 57–93. [CrossRef]
48. Aggarwal, M.D.; Batra, A.K.; Lal, R.B.; Penn, B.G.; Frazier, D.O. Growth and Characteristics of Bulk Single Crystals Grown from Solution on Earth and in Microgravity. Available online: <https://ntrs.nasa.gov/archive/nasa/casi.ntrs.nasa.gov/20110006347.pdf> (accessed on 10 August 2019).
49. Liu, Z.; Zhao, Q.; Wei, L.; Wu, D.; Ma, L. Effect of struvite seed crystal on map crystallization. *J. Chem. Technol. Biot.* **2011**, *86*, 1394–1398. [CrossRef]
50. Ruan, Z.Y.; Tian, Y.X.; Ruan, J.F.; Cui, G.J.; Iqbal, K.W.; Iqbal, A.; Ye, H.R.; Yang, Z.Z.; Yan, S.Q. Synthesis of hydroxyapatite/multi-walled carbon nanotubes for the removal of fluoride ions from solution. *Appl. Surf. Sci.* **2017**, *412*, 578–590. [CrossRef]
51. Chesne, R.B.; Kim, C.S. Erratum to: Zn (II) and Cu (II) adsorption and retention onto iron oxyhydroxide nanoparticles: Effects of particle aggregation and salinity. *Geochem. Trans.* **2015**, *16*, 17. [CrossRef]

